Manuscript Details

Manuscript number	GEODER_2018_52
Title	Relating soil C and organic matter fractions to structural stability
Article type	Research Paper

Abstract

Soil organic matter (SOM) is important for maintaining soil structural stability (SSS). The influence of soil organic carbon (SOC) and different organic matter components on various SSS measures were quantified. We used a silt loam soil with a wide range of SOC (0.0080-0.0427 kg kg-1 minerals) sampled in spring 2015 from the Highfield Ley-Arable Long-Term Experiment at Rothamsted Research. Four treatments were sampled: Bare fallow, continuous arable rotation, ley-arable rotation, and grass. Soils were tested for clay dispersibility (DispClay), clay-SOM disintegration (DI, the ratio between clay content without and with SOM removal) and dispersion of particles <20 μm. The SSS tests were related to SOC, permanganate oxidizable carbon (POXC), hot water-extractable carbon (HWC), mid-infrared photoacoustic spectroscopy (FTIR-PAS) and mineral fines/SOC ratio. SSS increased with increasing content of SOM components. The relationships between SOM components and SSS followed a broken-stick regression with a change point at ~0.0230 kg SOC kg-1 minerals (clay/SOC~10) coinciding with a change from the tilled treatments to the grass treatment. We found a greater influence of SOC, POXC and HWC on SSS at contents below the change point than above. A stronger linear relation between POXC and DispClay compared to SOC and HWC suggests that POXC was a better predictor of the variation in DispClay. POXC and HWC were less related to DI than SOC. The grass treatment had a very stable structure, shown in all SSS tests, probably due to the absence of tillage and large annual inputs of stabilizing agents. This suggests that a change in management from arable rotation to permanent grass is an effective tool for improving SSS.

Keywords	soil structural stability; soil organic carbon; permanganate oxidizable carbon; hot water-extractable carbon; soil management

Corresponding Author	Johannes Lund Jensen
Corresponding Author's Institution	Aarhus University - Department of Agroecology
Order of Authors	Johannes Lund Jensen, Per Schjønning, chris chris.watts@rothamsted.ac.uk, Bent T. Christensen, Clément Peltre, Lars Munkholm

Suggested reviewers	Mike Beare, Hugh Riley, Denis Angers, Cassio Antonio Tormena, Pascal Boivin

Submission Files Included in this PDF

File Name [File Type]

Cover_Letter.docx [Cover Letter]

Highlights.docx [Highlights]

Manuscript.docx [Manuscript File]

Appendix A. Supplementary figures.docx [e-Component]

To view all the submission files, including those not included in the PDF, click on the manuscript title on your EVISE Homepage, then click 'Download zip file'.

Johannes Lund Jensen
PhD Student
Soil Physics and Hydropedology
Dept. of Agroecology
Faculty of Science and Technology
Aarhus University
Blichers Allé 20
DK-8830 Tjele, Denmark

Mobile: +45 2636 0847
jlj@agro.au.dk
http://agro.au.dk/en/research/sektioner/soil-physics-and-hydropedology/

January 18th, 2018

To the Editorial Board of *Geoderma*,

Please consider the attached manuscript entitled "**Relating soil C and organic matter fractions to structural stability**" by Jensen et al. for review and publication in *Geoderma*. It describes original research not published elsewhere and not submitted for publication in other journals.

Soil organic matter (SOM) is important for maintaining soil structural stability (SSS).The current study relates a number of SOM components to various SSS tests using contrasting treatments from the Highfield Ley-Arable Long-Term Experiment at Rothamsted Research (UK). This was done without confounding effects of soil type, soil texture, and climate. The results showed that the relationships between SOM components and SSS followed a broken-stick regression with a change point coinciding with a change from the tilled treatments to the grass treatment. The effect of increasing SOM components on SSS was greater below the change point, i.e. at low contents. The grass treatment had a very stable structure indicating that changing management from arable rotation to permanent grass is an effective tool for improving SSS.

If you have any further questions regarding our manuscript submission, please do not hesitate to contact me.

Sincerely,
Johannes Lund Jensen

Highlights

- Soil structural stability increased with an increase in SOM components
- The effect of increasing SOM components was greater at low contents
- The change point for soil structural stability was at a clay/SOC ratio close to 10
- Grassland soil has a very stable structure compared to tilled soil

Relating soil C and organic matter fractions to structural stability

Johannes L. Jensen*[1], Per Schjønning[1], Christopher W. Watts[2], Bent T. Christensen[1], Clément Peltre[3], Lars J. Munkholm[1]

[1] Department of Agroecology, Aarhus University, Blichers Allé 20, 8830 Tjele, Denmark

[2] Department of Sustainable Agriculture Sciences, Rothamsted Research, Harpenden, Hertfordshire AL5 2JQ, United Kingdom

[3] Department of Plant and Environmental Sciences, University of Copenhagen, Thorvaldsensvej 40, 1821 Frederiksberg, Denmark

* Corresponding author

E-mail address: jlj@agro.au.dk (J. L. Jensen).

Type of Paper: Original research paper

Number of figures: 6

Number of tables: 3

Submitted to Geoderma the 18th of January 2018

ABSTRACT

Soil organic matter (SOM) is important for maintaining soil structural stability (SSS). The influence of soil organic carbon (SOC) and different organic matter components on various SSS measures were quantified. We used a silt loam soil with a wide range of SOC (0.0080-0.0427 kg kg^{-1} minerals) sampled in spring 2015 from the Highfield Ley-Arable Long-Term Experiment at Rothamsted Research. Four treatments were sampled: Bare fallow, continuous arable rotation, ley-arable rotation, and grass. Soils were tested for clay dispersibility (DispClay), clay-SOM disintegration (DI, the ratio between clay content without and with SOM removal) and dispersion of particles <20 μm. The SSS tests were related to SOC, permanganate oxidizable carbon (POXC), hot water-extractable carbon (HWC), mid-infrared photoacoustic spectroscopy (FTIR-PAS) and mineral fines/SOC ratio. SSS increased with increasing content of SOM components. The relationships between SOM components and SSS followed a broken-stick regression with a change point at ~0.0230 kg SOC kg^{-1} minerals (clay/SOC~10) coinciding with a change from the tilled treatments to the grass treatment. We found a greater influence of SOC, POXC and HWC on SSS at contents below the change point than above. A stronger linear relation between POXC and DispClay compared to SOC and HWC suggests that POXC was a better predictor of the variation in DispClay. POXC and HWC were less related to DI than SOC. The grass treatment had a very stable structure, shown in all SSS tests, probably due to the absence of tillage and large annual inputs of stabilizing agents. This suggests that a change in management from arable rotation to permanent grass is an effective tool for improving SSS.

Keywords: soil structural stability; soil organic carbon; permanganate oxidizable carbon; hot water-extractable carbon; soil management

Abbreviation: A, Continuous arable rotation; BF, Bare fallow; CEC, Cation exchange capacity; DI, Clay-SOM disintegration; DispClay, Clay dispersibility; DispFines20, Dispersion of particles <20 μm; Fines20, Mineral particles <20 μm; FTIR-PAS, Mid-infrared photoacoustic spectroscopy; G, Grass; HWC, Hot water-extractable carbon; LA, Ley-arable rotation; LF-free-SOC, Light fraction-free-SOC; LFSOC, Light fraction organic carbon; NTU, Nephelometric turbidity unit; PCA, Principal component analysis; POXC, Permanganate oxidizable carbon; SSA, Specific surface area; SSS, Soil structural stability.

1. Introduction

The importance of soil organic matter (SOM) on key soil properties and functions is well-known (e.g., Johnston et al., 2009), and as a consequence loss of SOM is considered as a major threat to sustained soil functions (Amundson et al., 2015). One soil property affecting key soil functions is soil structure. Soil structure is the relative arrangement of particles and pores (Dexter, 1988), and the ability of soil structure to resist external stresses both mechanical and or from water is soil structural stability (SSS). Greater SSS is essential for minimizing the risk of downward transport of fine particles carrying pollutants to the water environment (de Jonge et al., 2004), soil erosion (Le Bissonnais, 1996), soil cementing and seedbeds with hard and non-friable aggregates (Kay and Munkholm, 2004). SOM content is an important factor affecting SSS (Bronick and Lal, 2005), and a range of studies have shown that an increase in SOM content increases SSS (e.g., Jensen et al., 2017a; Watts and Dexter, 1997).

Soil organic carbon (SOC) is the main constituent of SOM and since an increase in SOC content generally increases SSS it may serve as a proxy for SSS. Labile organic compounds are considered readily decomposable, and are potentially better indicators for soil functions (Haynes, 2005). For example, permanganate oxidizable carbon (POXC) is considered a processed labile component of SOM and has been found to be more sensitive to differences in management than total SOC (Culman et al., 2012). POXC is easy and cheap to measure, and has been suggested as the best single predictor of soil health (Fine et al., 2017) and as a better predictor of crop productivity than total SOC (Hurisso et al., 2016). Similarly, hot water-extractable carbon (HWC) has been highlighted as a soil quality indicator more sensitive to management changes than total SOC (Ghani et al., 2003). HWC is considered a labile component of SOM consisting of microbial and plant derived material (Hirsch et al., 2017; Villada et al., 2016). Another measure, which potentially could better explain changes in SSS than total SOC could be to subtract light fraction organic

carbon (LFSOC) from total SOC since LFSOC is a fraction not closely associated to mineral particles (Gregorich et al., 2006). Mid-infrared photoacoustic spectroscopy (FTIR-PAS) can be used to assess differences in SOM quality (Peltre et al., 2014; Peltre et al., 2017), which potentially could improve the explanatory power in predicting SSS.

Increasing evidence suggest that soils exhibit a capacity factor for carbon sequestration also known as saturation state (Hassink, 1997; McNally et al., 2017). The saturation state of the soil has been found to influence the SSS measure, clay dispersibility, rather than SOC *per se* (Dexter et al., 2008). The saturation state has been assessed through the clay/SOC ratio, and a critical value close to 10 corresponding to a soil where the mineral particles are saturated with SOC has been found in several studies (Dexter et al., 2008; Getahun et al., 2016; Jensen et al., 2017a; Schjønning et al., 2012). Soils with clay/SOC>10 may thus be considered SOC-unsaturated, and for such soils SSS may be reduced. A similar threshold has been found for mineral particles <20 μm (Fines20) where the ratio of Fines20/SOC>20 indicates less SSS. Consequently, these mineral fines to SOC ratios may serve as soil type independent threshold values for SSS.

Previous studies often rely on samples retrieved from contrasting sites with different soil types and textures making quantification of the effect of SOM components on SSS dubious. This because the effects on SSS can be affected by other aggregate forming factors. More knowledge on the quantitative importance of SOM components on SSS using different pretreatments and energy input in the tests are needed.

The objective of this study was to quantify the influence of SOC on soil structural stability parameters determined in different ways and to test if knowledge about SOM characteristics could improve the predictive ability. A wide range of measures for the determination of SSS exists ranging in sample preparation, pretreatment, degree of disturbance and quantification (Le Bissonnais, 1996; Pojasok and Kay, 1990; Pulido Moncada et al., 2015). In this study, we applied

stability tests varying in pretreatment and ranging from low to very high degree of disturbance for a comprehensive evaluation of SOC effects on SSS. Soil was retrieved from the Highfield Ley-Arable Long-Term Experiment at Rothamsted Research (Highfield-LTE), a silt loam with a relatively homogeneous topsoil texture and a large gradient in SOC that has developed during at least 56 years of contrasting management practices without the confounding effects of soil type, soil texture and climate. Treatments were selected to obtain the widest possible gradient in SOC content, and thus ensuring major differences in SOM components.

2. Materials and methods

2.1 The Highfield-LTE and treatments

The Highfield-LTE was established in 1949 on a silt loam soil (Table 1) at Rothamsted Research, Harpenden, UK (51°80'N, 00°36'W) in a field that had been under permanent grass for centuries. The soil belongs to the Batcombe series, and the parent material include a relatively silty (loess-containing) superficial deposit overlying and mixed with clay-with-flints (Avery and Catt, 1995). The soil is classified as an Aquic Paludalf (USDA Soil Taxonomy System) and Chromic Luvisol (WRB) (Watts and Dexter, 1997). Average annual temperature and precipitation are 10.2ºC (mean of 1992-2014) and 718 mm (mean of 1981-2010), respectively (Scott et al., 2014).

We selected three treatments in the ley-arable experiment:
Continuous arable rotation (A), winter cereals (winter wheat, *Triticum aestivum* L. and winter oats, *Avena sativa* L.) fertilized with 220 kg N ha^{-1} y^{-1} and maintained under standard Rothamsted farm practice with straw removed. Ley-arable rotation (LA), three-year grass/clover ley (meadow fescue, *Festuca pratensis* L.; timothy-grass, *Phleum pratense* L.; white clover, *Trifolium repens* L.) followed by three years arable (managed as A). The grass/clover ley received no N and was cut and

119 removed in early summer. The small amount of regrowth was topped in early autumn and left on
120 the plots. Two of the sampled plots were drilled with winter cereals following three years of
121 grass/clover, whereas the other two were drilled with grass/clover following three years of winter
122 cereals. Grass (G), ploughed and reseeded to grass (predominantly rye grass, *Lolium perenne* L.)
123 when the experiment was established (1949). The grass was managed as the grass/clover ley in LA.

124 We also selected the bare fallow (BF) treatment, which is not part of the original ley-arable
125 experiment and located adjacent to the ley-arable experiment (denoted Highfield bare fallow and
126 Geescroft bare fallow). The BF treatment has been maintained free of plants by regular tillage
127 (ploughed or rotavated two to four times a year) since 1959. The ploughing depth in BF, A and LA
128 was 0.23 m. The A, LA and G plots were fertilized with 65 kg P ha^{-1} and 250 kg K ha^{-1} every three
129 years.

130 The A, LA and G treatments were part of a randomized block design with four field
131 replicates, whereas the four BF plots were located at one end of the experiment (Fig. 1). The
132 dimensions of the LA plots were 50 m x 7 m, whereas it was 10 m x 6 m for the other plots. The A,
133 LA and G plots were smaller since they were part of a reversion experiment initiated in 2008. For
134 more details see Johnston (1972) and the electronic Rothamsted Archive
135 (www.era.rothamsted.ac.uk).

136 *2.2 Soil sampling*

137 Soil was sampled in March 2015 at field capacity water conditions (corresponding
138 approximately to a soil water potential of -100 hPa). Soil blocks (2750 cm^3) were sampled from the
139 6-15-cm soil layer by careful use of a spade. Three sampling sites in each experimental plot were
140 randomly chosen and labeled subplot. One of these blocks was extracted from each subplot adding
141 up to three blocks per plot. The soil was kept in rigid containers to prevent soil disturbance during
142 transport and stored in a field-moist condition at 2ºC until required. Soil from the blocks at subplot

level were spread out in steel trays at room temperature, carefully fragmented by hand in several sittings along natural planes of weakness and finally left to air-dry.

2.3 Basic chemical and physical analysis

Soil texture of air-dried bulk soil (crushed and passed through a 2-mm sieve) was determined by the hydrometer method for clay (<2 μm) and silt (2-20 μm) content and the sieve method for mineral particles >63 μm (Gee and Or, 2002). The soil was tested for $CaCO_3$ by adding a few droplets of 10% HCl, but none was found. SOM was removed by H_2O_2 before estimation of clay and silt as described in Jensen et al. (2017b). The SOC content was determined on ball-milled subsamples using dry combustion (Thermo Flash 2000 NC Soil Analyzer, Thermo Fisher Scientific, Waltham Massachusetts, USA). Specific surface area (SSA) was determined by the ethylene glycol monoethyl ether method (Petersen et al., 1996), and cation exchange capacity (CEC) was determined after Kalra and Maynard (1991). Soil pH was determined in 0.01 M calcium chloride ($CaCl_2$) solution (1:2.5, *w*/w). Clay, silt and SOC content were determined at subplot level, whereas the other properties were determined at plot level.

2.4 Soil organic matter characteristics

Permanganate oxidizable carbon (POXC) was determined at subplot level following Culman et al. (2012). Air-dry 2-mm sieved soil equivalent to 2.5 g oven-dry weight was weighed into a 50 ml falcon tube, and was shaken in 18.0 ml of distilled water and 2.0 ml 0.2 M potassium permanganate ($KMnO_4$) with pH 7.2 at 33 rpm for 2 min. After shaking, the soil was allowed to settle for 10 min after which 0.5 ml of the supernatant was transferred to falcon tubes containing 49.5 ml of water. The absorbance of the diluted solution was measured at 550 nm using a spectrophotometer (Thermo Electron Spectronic Helios Alpha Beta UV-visible). Absorbance of

four standard stock $KMnO_4$ solutions were measured to create a standard curve, and the absorbance of the samples were converted to POXC using the equation of Weil et al. (2003).

Hot water-extractable carbon (HWC) was determined at subplot level following Ghani et al. (2003). Briefly, air-dry 2-mm sieved soil equivalent to 3 g oven-dry weight was weighed into a 50 ml falcon tube, and was shaken in 30 ml distilled water at 33 rpm for 30 min, at 20ºC. After centrifugation (3500 rpm, 20 min) the supernatant was decanted, soil resuspended and shaken for 16 h at 200 rpm, at 80ºC. After centrifugation, the supernatant was transferred to 50 ml maxi-spin filter tubes equipped with a cellulose acetate membrane filter (0.45 µm pore size), filtered by centrifugation for 10 min at 3000 rpm and carbon determined by wet oxidation using a Shimadzu TOC-V analyzer.

Fractionation based on density was determined at subplot level using a modification of the method described by Sohi et al. (2001). Briefly, 10 g of air-dried 2-mm sieved soil was weighed into a 50 ml falcon tube, 35 mL of NaI solution with a density of 1.8 g cm^{-3} was added, and the solution was shaken at 33 rpm for 2 h. The suspension was centrifuged for 30 min after which floating particles was transferred to a glass fiber filter (type GF/A, 110 mm diam., 1.6 µm retention, Whatman International, Kent, UK), and filtered under suction in a vacuum filtration unit (Büchner funnel). The light fraction organic matter (LFOM) retained on the filter was washed carefully and transferred to a crucible. To ensure a quantitative removal of LFOM the procedure was repeated. The remaining heavy fraction (HF) was washed three times and transferred to a large crucible. The oven-dry weight of the LF and HF were estimated by drying (105 °C for 24 h). The amount of OM recovered was estimated by loss-on-ignition (LOI; 500 °C for 4 h) both for the LFOM and HF. A 5 g air-dry bulk soil sample was dried to allow expressing results on an oven-dry basis after which LOI was determined. The LOI of bulk soil was used to make a model to predict the SOC of the HF

188 based on a multiple regression of SOC against LOI and clay (Model H2.1, Table 2 in Jensen et al.,
189 2018):

190 SOC = 0.515 LOI (P<0.001) - 0.043 Clay (P<0.001), (n=48, R^2= 0.990) (1)

191 Ten tests without soil (blind tests) were performed. The blind test estimate was subtracted
192 from the LFOM estimate. The LFOM was converted to LFSOC by multiplying with 0.515 (Eq. 1),
193 expressed as percentage of the sum of LFSOC and HFSOC, and normalized to the measured SOC
194 content. Light fraction-free-SOC (LF-free-SOC) was calculated by subtracting LFSOC from SOC.

195 Fourier transform mid-infrared photoacoustic spectroscopy (FTIR-PAS) was determined at
196 plot level following Peltre et al. (2014). Air-dry 2-mm sieved soil samples were ball-milled and
197 packed in 10-mm diameter cups and functional groups of soil components were investigated using a
198 Nicolet 6700 FTIR spectrometer (Thermo Scientific) equipped with a PA301 photoacoustic detector
199 (Gasera Ltd. Turku, Finland). Spectra were recorded with an average of 32 scans within the range
200 4000-600 cm^{-1} and with 2 cm^{-1} intervals. A flow of helium was used as purge gas to remove noise
201 produced by ambient moisture and CO_2 as well as moisture from the sample after insertion of the
202 cup in the photoacoustic detector chamber. We focused on the 1700-1300 cm^{-1} region to reduce
203 overlapping from bands arising from soil minerals. The spectral peak area between 3000 and 2800
204 cm^{-1} were integrated as described in Peltre et al. (2017), and reflects the amount of aliphatics in the
205 soil (Leifeld, 2006).

206 *2.5 Soil structural stability*

207 Clay dispersibility (DispClay) was determined at subplot level on 1-2 mm aggregates
208 extracted from the air-dry 2-mm sieved soil. The aggregates were adjusted to a matric water
209 potential of -100 hPa as described in Schjønning et al. (2012). In short, the aggregates were put on a

210 tension table at -100 hPa, gradually exposed to reduced suctions until -3 hPa, and finally
211 equilibrated at -100 hPa by gradually increased suctions. The rewetting was done with great caution
212 to avoid air explosion (slaking). Artificial rainwater was added to cylindrical plastic bottles
213 containing 10 g of aggregates in order to obtain a soil:water ratio of 1:8 by weight. After end-over-
214 end rotation (33 rpm, 23-cm diameter rotation) for 2 min, the bottles were left to stand for 230 min,
215 after which the upper 50 mm (60 ml) containing particles ≤2 μm was siphoned off. The weight of
216 dispersed clay was determined after oven-drying (105 °C for 24 h) and corrected for particles >250
217 μm isolated by chemical dispersion.
218 Dispersion of particles <20 μm (DispFines20) was measured at different time steps at plot
219 level on field-moist soil. Soil was retrieved from the minimally-disturbed soil cubes using a small
220 corer (22-mm diameter) and gently crumbled by hand to pass an 8-mm sieve. Artificial rainwater
221 was added to a cylindrical bottle containing soil equivalent to 1 g oven-dry weight to obtain a
222 soil:water ratio of 1:100 by weight. The bottle was end-over-end rotated (33 rpm, 23-cm diameter
223 rotation) for 2, 4, 8, 16, 32, 64 and 128 min. At each time step the bottle was left to stand for 67 sec,
224 after which the upper 30 ml containing particles <20 μm was siphoned off and turbidity of the
225 suspension was measured on a Hach 2100AN turbidimeter (Hach, Loveland, CO). After the
226 turbidity measurements taken at time steps 2-64 min the soil suspension was transferred back to the
227 bottle. Thus, the measurements at the different time steps was done on the same sample. After the
228 final measurement, the 30 ml was transferred to a beaker and bulked at treatment level. For each
229 treatment, correlations between nephelometric turbidity unit (NTU) and particle concentration were
230 made by doing dilution series. The calibration curves can be seen in Fig. S1 in Supplementary
231 material. The results were corrected for particles > 250 μm isolated by chemical dispersion.

232 Soil samples at subplot level were analyzed without H_2O_2-removal of SOM before estimation
233 of clay as described in Jensen et al. (2017b), and clay-SOM disintegration (DI) was calculated as
234 the ratio between clay content estimated without SOM removal and with removal. Soil with DI
235 values <1 kg kg^{-1} can be interpreted as extremely stable since they have resisted disintegration after
236 end-over-end rotation for 18 h in sodium pyrophosphate.

237 *2.6 Calculations and statistics*

238 The soil components measured in the paper are given as fractions of oven-dry weight (105ºC
239 for 24 h) of the SOM-free mineral fraction. This includes mineral particle size fractions, SOC,
240 POXC, HWC, LF-free-SOC, SSA, CEC and DispClay. DispFines20 is given as a fraction of SOM-
241 free mineral fraction <20 μm.

242 The statistical analysis and processing of spectral data applied the R-project software package
243 Version 3.4.0 (R Foundation for Statistical Computing). Treatment effects for the comparison of A,
244 LA and G were analyzed with a linear mixed model including block as a random effect. The
245 criterion used for statistical significance of treatment effects was $P<0.05$. When the treatment effect
246 was significant, further analyses were made to isolate differences between treatments (pairwise
247 comparisons) using the general linear hypotheses (*glht*) function implemented in the R *multcomp*
248 package and the Kenward-Roger method to calculate degrees of freedom (Kenward and Roger,
249 2009). Treatment differences for the comparison of BF and the other treatments were calculated
250 based on a pairwise *t*-test, acknowledging that this is a less robust test, and that the treatment
251 differences could be due to soil variation since the BF treatment is not a part of the ley-arable
252 experiment. Inverse transformation was performed on DispFines20 to stabilize the variance. The
253 broken-stick model was fitted using the *segmented* package in R. A piece-wise linear model was
254 used:

255 $y = \beta_0 + \beta_1(x) + \beta_2(x\text{-}c)^+ + e$ (2)

256 where y is the dependent variable, x is the independent variable, c is the change point and e is the
257 residual standard error (Toms and Lesperance, 2003). The $^+$ sign indicates that the last term only is
258 valid when $x>c$.

259 Spectral data processing included baseline correction, smoothing using a Savitzky-Golay filter
260 calculated on three data points on each side with a zero-order polynomial, and normalization by the
261 average absorbance on the whole spectra. Principal component analysis (PCA) on the FTIR-PAS
262 spectra was performed using the *ade4* package in R.

263

264 **3. Results**

265 *3.1 Basic soil characteristics*

266 Differences in the contents of clay, silt and sand were in general not significant between
267 treatments (Table 1) and the effect of the contrasting management practices could be investigated
268 without confounding effects related to soil texture. SSA differed significantly following the same
269 pattern as SOC. CEC was significantly higher for G compared to the BF treatment, and the amount
270 of exchangeable Ca^{2+} was significantly higher for G compared to the other treatments. Soil pH was
271 not affected by the contrasting management practices.

272 *3.2 Soil organic matter characteristics*

273 Concentration of SOC differed significantly in the order G>LA=A>BF (Table 2). POXC,
274 HWC, LFSOC, and the aliphatic C-H peak area (3000-2800 cm^{-1}) followed the treatment
275 differences in SOC. The full spectral range as well as the SOM fingerprint region (1700-1300 cm^{-1})
276 at plot level can be seen in Supplementary material, Figs. S2 and S3, respectively.

277 The aliphatic peak area normalized by the SOC content was higher in the BF than the G
278 treatment indicating that SOM in G soil was more depleted in aliphatics. The POXC contributed to
279 1.7, 2.6, 2.8 and 2.5 % of total SOC, respectively, and the HWC in BF, A, LA and G contributed to
280 4.6, 4.5, 5.0 and 4.9 % of total SOC, respectively. The increase in POXC with an increase in SOC
281 was different for the G treatment compared to A and LA (Fig. 2a). The narrow range in SOC
282 content for BF did not allow an evaluation of the POXC-SOC relation within the SOC-depleted BF
283 soil, but the first slope of the broken-stick model was similar to a linear regression with only A and
284 LA (35.4 compared to 33.9 g kg^{-1} SOC). This indicates that the level of POXC for BF was in line
285 with the trend of the other tilled treatments (A and LA). The x-intercept of the broken-stick model
286 in Fig. 2a was 0.00458 kg SOC kg^{-1} minerals, and suggests that no POXC was oxidized at and
287 below this SOC content. For the wide range in SOC in this study, HWC correlated linearly to SOC
288 with an intercept value close to zero (Fig. 2b). Our data thus point to a concentration of ~0.05 kg
289 HWC per kg SOC (~5%) irrespective of SOC level.
290 The PCA analysis based on the 1700-1300 cm^{-1} region clearly separated the treatments on the
291 first principal component (PC1) explaining 84.6% of the spectral variance (Fig. 3a). Field plots
292 from the G and BF treatment were located on the left and right side of the PCA plane, respectively.
293 Field plots from the A and LA treatments were in the center of the PCA plane and did not differ
294 much. Examination of the loading of PC1 indicated that BF soils were relatively enriched in organic
295 compounds vibrating in the range between 1700 and 1580 cm^{-1} with a peak at 1625 cm^{-1} (Fig. 3b).
296 Absorption in this region is attributed to vibration of aromatics and carboxylate at 1600-1570 cm^{-1},
297 amine at 1610 cm^{-1}, clay-bound water at 1640 cm^{-1}, aromatics at 1660-1600 cm^{-1} and amides at
298 1670-1640 cm^{-1} (Table 1 in Peltre et al., 2017). In contrast, G soils were relatively enriched in
299 organic compounds vibrating in the range between 1580-1495 cm^{-1} and 1475-1325 cm^{-1} with peaks
300 at 1550, 1510 and 1385 cm^{-1} (Fig. 3b). These regions are attributed to vibration of nitrate at 1380

301 cm^{-1}, carboxylate at 1390 cm^{-1}, amide III at 1420 cm^{-1}, carbonates at 1430 cm^{-1}, aliphatic methyls at
302 1445-1350 cm^{-1}, lignin rings at 1505-1515 cm^{-1} and amide II at 1570-1540 cm^{-1} (Table 1 in Peltre et
303 al., 2017).

304 *3.3 Soil structural stability*

305 The amount of dispersible clay differed significantly in the order BF>A>LA>G, and the
306 disintegration of soil without SOM removal was significantly lower for the G treatment compared
307 to the other treatments (Table 2). Linear, semi-logarithmic and broken-stick models were employed
308 to describe the correlations of SOC, POXC and HWC to DispClay and DI (Table 3). The coefficient
309 of determination (R^2) was highest when DispClay and DI were related to SOC with a broken-stick
310 model (see relation on Fig. 4a). Similar relationships were found when relating POXC and HWC to
311 DispClay and DI (Figs. 4b and 4c).

312 Relating changes in DispClay to LF-free-SOC did not improve R^2 compared to SOC (Fig. 5a),
313 whereas LF-free-SOC increased the explained variation in DI by 1 %-unit (Fig. 5b).

314 DispFines20 was significantly lower for the G treatment compared to the other treatments at
315 all time steps (Fig. 6a), and the release-curve had a contrasting shape compared to the other
316 treatments. DispFines20 was significantly lower for the LA than the A treatment after both 64 and
317 128 min. The release rate was markedly higher in the beginning for BF, A and LA compared to G
318 (Fig. 6b). From approx. 24 min onwards, G had a higher release rate compared to the other
319 treatments. At all time steps, DispFines20 was virtually constant across the four G treatment plots
320 despite a range in SOC, while considerable variation was observed for the narrower SOC ranges of
321 the other three treatments (Fig. S4 in Supplementary material).

322

323 **4. Discussion**

4.1 Linking soil organic matter components to soil structural stability

POXC has been promoted as a relatively processed or stabilized pool of active SOC (Culman et al., 2012), and as organic material to support biological functions (Idowu et al., 2008), while HWC has been promoted as an indicator of soil biochemical quality (Ghani et al., 2003). Both SOM fractions are considered labile and sensitive indicators for assessing management-induced changes (Culman et al., 2012; Ghani et al., 2003). Labile organic compounds are known to bond mineral particles together and thus stabilize them against mechanical damage (Degens, 1997). However, this mechanism would not be expected to play any role for the clay-SOM disintegration (DI) test that involves a rather extreme disruptive energy to soil structural units (end-over-end shaking for 18 h in sodium pyrophosphate solution). In accordance with this, we note a higher coefficient of determination in the broken-stick regression relating DI to SOC (R^2=0.88) than for POXC and HWC (R^2=0.82 and R^2=0.79, respectively). One may speculate that stable organo-mineral associations (i.e. at submicro-aggregate and primary particle scale) are causing the extreme stability at high SOC contents. The similar pattern observed for POXC and HWC (broken-stick) then relates to the near linear relations observed between total SOC and these two fractions (Fig. 2).

For the DispClay SSS measure, we observe nearly identical coefficients of determination in the broken-stick models describing the data: R^2 equals 0.94, 0.93 and 0.91 with SOC, POXC and HWC as predictor (Table 3). We further note that the broken-stick is "less broken" especially when using POXC as predictor of trends in data (slope ratios, Table 3). This observation is supported by a higher ability of POXC to describe data in a linear model (R^2=0.91) compared to HWC and SOC (R^2=0.82 and R^2=0.84, respectively). Overall, this may indicate that POXC is superior to SOC and HWC in describing the variation in DispClay.

Our study does not allow a definite clarification regarding which mechanisms are in play in SSS. The indication that POXC is superior in describing the variation in DispClay may be related to

a link to bonding agents such as polysaccharides, which are assumed predominantly active at micro-aggregate scale (Tisdall and Oades, 1982). However, the composition of POXC is unknown, which is related to the destruction of the fraction by oxidization. The lower predictive ability of HWC to explain SSS data and its close correlation to SOC may indicate that it is a too simplistic quality characteristic of SOC. Other studies have emphasized the need to focus on the carbohydrate-C contents in the hot water-extracts (e.g., Haynes, 2005), and studies have shown that hot water-extractable carbohydrate-C was a better predictor of SSS than SOC (Haynes and Swift, 1990).

Changes in DispClay and DI may be better explained by LF-free-SOC than total SOC. However, the difference in using LF-free-SOC compared to SOC was marginal (Fig. 5). The decrease in DispClay and DI when going from BF to G could be related to a general enrichment in aliphatics and lignin, and a decrease in carboxylic groups and amides (Table 2, Fig. 3). The higher amount of carboxyl-rich and amide-rich SOM suggest that the SOM in the BF soils were more oxidized being in agreement with the findings of Barré et al. (2016). Such compounds have been related to microbial processed and stable SOM in organo-mineral associations (Kleber et al., 2015). A higher proportion of aliphatics in SOM from the BF soils also support the presence of a more decomposed SOM. The results indicate that plant residues were decomposed rapidly in the BF soils leaving behind SOM enriched in microbial processed OM. In contrast, less oxidized and continually renewed compounds accumulated in the G soils.

4.2 Management system effects on soil structural stability

The four treatments can be seen as three management systems comprising the BF treatment with intensive tillage, no plants or carbon input, the A and LA treatments with plants and tillage, and the G treatment with plants and absence of tillage. The G treatment differed from the other treatments by having a very stable structure and a better ability to resist increasing degrees of

371 disturbance. Consequently, the potential maximum SSS was only fully achieved for the long-term G
372 treatment. This was reflected in the DispClay and DI tests where the change point of the broken-
373 stick model for SOC content was confounded with treatment, and represented a change from the LA
374 to G treatment (Fig. 4a). Also the results on DispFines20 support a change in stability between the
375 G treatment and the other treatments illustrated by the contrasting curve, release rate and higher
376 stability at all time steps (Fig. 6). Permanent grass stands out from the other treatments by having a
377 greater input of above- and belowground plant residues. Hirsch et al. (2009, 2017) found a
378 markedly greater number of roots and mesofauna in G compared to BF and A, and a larger
379 abundance of fungi. Roots and fungal hyphae can act as binding agents, enmesh aggregates
380 (Elmholt et al., 2008; Tisdall and Oades, 1982), and potentially increase SSS, and mesofauna can
381 contribute to stability via stabilizing decomposition products (Oades, 1993). In addition, the effect
382 of these stabilizing agents are persistent since they are continuously replaced, and remain
383 undisturbed due to the absence of tillage. The limited effect of SOC on DispFines20 within the G
384 treatment at all time steps (Fig. S4 in Supplementary material) may be related to the larger scale
385 applied in the test, i.e. whole-soil samples not broken down to more than 8 mm. At a larger scale,
386 management system drivers such as macro-aggregate stabilizing agents seemed to be more distinct,
387 while SOC played a minor role. The greater stability of the G treatment may also be related to the
388 absence of tillage shown to be detrimental to the preservation of stabilizing agents.

389 The higher amount of soluble Ca^{2+} ions in the G treatment increases the tendency of clay
390 particles to flocculate (Le Bissonnais, 1996), and may also contribute to the higher stability.
391 However, the importance of cations for aggregate stability is considered less important in soil high
392 in clay or SOC (Bronick and Lal, 2005). Matthews et al. (2008) found a decrease in wettability for

393 G, whereas wettability was similar for BF, A and LA treatments. Thus, the very stable structure of
394 the G soil may also be partially related to decreased wettability.

395 *4.3 Critical carbon levels*

396 Our SSS measures DI and DispClay showed a change in the relation to SOC at around 0.0230
397 kg kg^{-1} minerals for this soil (broken-stick change point; Fig. 4a). The carbon saturation concept
398 (Six et al., 2002; Stewart et al., 2007) implies the existence of a SOC concentration that for a given
399 soil provides a full "coverage" of the surface of soil minerals with SOC. This potential carbon
400 storage capacity (Ingram and Fernandes, 2001) was verified for a range of grassland soils assumed
401 saturated with organic carbon (Hassink, 1997). A SOC concentration of ~0.0230 kg kg^{-1} minerals
402 found in this study may thus be hypothesized to reflect the potential storage capacity for this soil.
403 The broken-stick pattern for DispClay indicates that SOC influences SSS more for soils with SOC
404 below the change point than above (Fig. 4a). DispClay increases more with reduction in SOC when
405 the soil is unsaturated with carbon (below the change point) than when it is saturated. This is in line
406 with Jensen et al. (2017a), who found SOC to be important for SSS for SOM-depleted soil.
407 Interestingly, the DI test with extreme energy input showed that all unsaturated soil samples
408 behaved similarly and fully disintegrate (slope not significantly different from zero; Fig. 4a).

409 The SOC threshold for a change in SOC effects on SSS differ from soil to soil, e.g. around
410 0.0110 kg SOC kg^{-1} minerals for a sandy loam in Denmark (Jensen et al., 2017a). Thus, SOC
411 critical to SSS seems soil type dependent. Dexter et al. (2008) and Jensen et al. (2017a) found an
412 increasingly compromised SSS when the clay/SOC ratio was above 10. Schjønning et al. (2012)
413 and Jensen et al. (2017a) found that a Fines20/SOC ratio of 20 serve as a similar critical threshold
414 value. The clay/SOC and Fines20/SOC ratios for a change in DispClay and DI were calculated by
415 dividing the average clay or Fines20 content with the change point giving values of 11 and 23,

416 respectively. Thus, our results support the soil clay/SOC~10 or Fines20/SOC~20 as defining factors
417 for SSS.

418 In this study the thresholds for changes in SOC (as well as POXC and HWC) effects on SSS
419 is confounded with management (Fig. 4). Thus the calculated soil mineral fines/SOC thresholds
420 may relate to a quantity of SOC as well as management system (as discussed in section 4.2). This
421 was unavoidable since systems with a wide range in SOC often will require contrasting
422 management. However, confounding effects derived from differences in soil type, soil texture and
423 climate were eliminated.

424

425 **5. Conclusions**

426 We exploited the unique range in SOM within Highfield, which has developed due to
427 contrasting long-term management practices. Soil structural stability (SSS) increased with an
428 increase in SOM components. However, the relationships followed a broken-stick regression with
429 the greater effect occurring when SOM components were less. The SOM fractions permanganate
430 oxidizable carbon (POXC) and hot water-extractable carbon (HWC) were less related to clay-SOM
431 disintegration than SOC. However, POXC seemed superior in describing the variation in clay
432 dispersibility compared to SOC and HWC. The permanent grass had a very stable structure - even
433 when exposed to high degree of disturbance. This may be ascribed to the management system,
434 which result in higher amount of stabilizing agents due to greater and annually renewed inputs of
435 above- and belowground plant residues as well as absence of tillage. Both aspects promote a high
436 abundance of soil microbiota and mesofauna. For this soil, management changes promoting SOM
437 content increased SSS up to a specific threshold coinciding with a change to permanent grass.
438 Consequently, increasing the SOC content at low contents or changing management from arable

rotation to permanent grass seem promising tools for improving SSS. Further, this study supports the existence of critical soil mineral fines/SOC ratios for SSS with change points at clay/SOC~10 and Fines20/SOC~20.

Acknowledgements

We gratefully acknowledge the technical assistance of Stig T. Rasmussen, Dept. Agroecology (Aarhus University), and the technical staff at Rothamsted Research. We thank Bodil B. Christensen, Palle Jørgensen, Karin Dyrberg, Kim M. Johansen, and Morgane Coulumbel for technical assistance. We thank Kristian Kristensen for statistical advice. The study was supported by the Green Development and Demonstration Programme (GUDP) of the Ministry of Environment and Food of Denmark through the "Cover crops for optimization of cereal based cropping systems" (Grant No. 3405-11-0225) and "Optimized soil tillage in cereal based cropping systems" (Grant No. 34009-12-0502) projects, and by the EU 7th Research Framework Programme, Distributed Infrastructure for Experimentation in Ecosystem Research (ExpeER) through the project "Identification of soil organic carbon thresholds for sustained soil functions in agroecosystems" (Grant No. 262060). The Rothamsted Long-term Experiments National Capability is supported by the UK Biotechnology and Biological Sciences Research Council (BBSRC) and the Lawes Agricultural Trust.

459 **References**

460 Amundson, R., Berhe, A.A., Hopmans, J.W., Olson, C., Sztein, A.E., Sparks, D.L., 2015. Soil and
461 human security in the 21st century. Science 348, 1261071.
462 Avery, B.W., Catt, J.A., 1995. The soils at Rothamsted. Lawes Agricultural Trust, 1-44.
463 Barré, P., Plante, A.F., Cécillon, L., Lutfalla, S., Baudin, F., Bernard, S., Christensen, B.T., Eglin,
464 T., Fernandez, J.M., Houot, S., Kätterer, T., Le Guillou, C., Macdonald, A., van Oort, F.,
465 Chenu, C., 2016. The energetic and chemical signatures of persistent soil organic matter.
466 Biogeochemistry 130, 1-12.
467 Bronick, C.J., Lal, R., 2005. Soil structure and management: a review. Geoderma 124, 3-22.
468 Culman, S.W., Snapp, S.S., Freeman, M.A., Schipanski, M.E., Beniston, J., Lal, R., Drinkwater,
469 L.E., Franzluebbers, A.J., Glover, J.D., Grandy, A.S., Lee, J., Six, J., Maul, J.E., Mirksy,
470 S.B., Spargo, J.T., Wander, M.M., 2012. Permanganate Oxidizable Carbon Reflects a
471 Processed Soil Fraction that is Sensitive to Management. Soil Sci. Soc. Am. J. 76, 494-504.
472 de Jonge, L.W., Kjaergaard, C., Moldrup, P., 2004. Colloids and Colloid-Facilitated Transport of
473 Contaminants in Soils. Vadose Zone J. 3, 321-325.
474 Degens, B.P., 1997. Macro-aggregation of soils by biological bonding and binding mechanisms and
475 the factors affecting these: a review. Aust. J. Soil Res. 35, 431-460.
476 Dexter, A., Richard, G., Arrouays, D., Czyż, E., Jolivet, C., Duval, O., 2008. Complexed organic
477 matter controls soil physical properties. Geoderma 144, 620-627.
478 Dexter, A.R., 1988. Advances in characterization of soil structure. Soil Tillage Res. 11, 199-238.
479 Elmholt, S., Schjønning, P., Munkholm, L.J., Debosz, K., 2008. Soil management effects on
480 aggregate stability and biological binding. Geoderma 144, 455-467.
481 Fine, A.K., van Es, H.M., Schindelbeck, R.R., 2017. Statistics, Scoring Functions, and Regional
482 Analysis of a Comprehensive Soil Health Database. Soil Sci. Soc. Am. J. 81, 589-601.

Gee, G.W., Or, D., 2002. Particle-size analysis. In: J.H. Dane, G.C. Topp (Eds.), Methods of Soil Analysis. Part 4 - Physical methods, Soil Science Society of America, Inc. Madison, Wisconsin, USA, 255-294.

Getahun, G.T., Munkholm, L.J., Schjønning, P., 2016. The influence of clay-to-carbon ratio on soil physical properties in a humid sandy loam soil with contrasting tillage and residue management. Geoderma 264, Part A, 94-102.

Ghani, A., Dexter, M., Perrott, K.W., 2003. Hot-water extractable carbon in soils: a sensitive measurement for determining impacts of fertilisation, grazing and cultivation. Soil Biol. Biochem. 35, 1231-1243.

Gregorich, E.G., Beare, M.H., McKim, U.F., Skjemstad, J.O., 2006. Chemical and Biological Characteristics of Physically Uncomplexed Organic Matter. Soil Sci. Soc. Am. J. 70, 975-985.

Hassink, J., 1997. The capacity of soils to preserve organic C and N by their association with clay and silt particles. Plant Soil 191, 77-87.

Haynes, R.J., 2005. Labile Organic Matter Fractions as Central Components of the Quality of Agricultural Soils: An Overview. Adv. Agron. 85, 221-268.

Haynes, R.J., Swift, R.S., 1990. Stability of soil aggregates in relation to organic constituents and soil water content. J. Soil Sci. 41, 73-83.

Hirsch, P.R., Gilliam, L.M., Sohi, S.P., Williams, J.K., Clark, I.M., Murray, P.J., 2009. Starving the soil of plant inputs for 50 years reduces abundance but not diversity of soil bacterial communities. Soil Biol. Biochem. 41, 2021-2024.

Hirsch, P.R., Jhurreea, D., Williams, J.K., Murray, P.J., Scott, T., Misselbrook, T.H., Goulding, K.W.T., Clark, I.M., 2017. Soil resilience and recovery: rapid community responses to management changes. Plant Soil 412, 283-297.

507 Hurisso, T.T., Culman, S.W., Horwath, W.R., Wade, J., Cass, D., Beniston, J.W., Bowles, T.M.,
508 Grandy, A.S., Franzluebbers, A.J., Schipanski, M.E., Lucas, S.T., Ugarte, C.M., 2016.
509 Comparison of Permanganate-Oxidizable Carbon and Mineralizable Carbon for Assessment
510 of Organic Matter Stabilization and Mineralization. Soil Sci. Soc. Am. J. 80, 1352-1364.
511 Idowu, O.J., van Es, H.M., Abawi, G.S., Wolfe, D.W., Ball, J.I., Gugino, B.K., Moebius, B.N.,
512 Schindelbeck, R.R., Bilgili, A.V., 2008. Farmer-oriented assessment of soil quality using
513 field, laboratory, and VNIR spectroscopy methods. Plant Soil 307, 243-253.
514 Ingram, J.S.I., Fernandes, E.C.M., 2001. Managing carbon sequestration in soils: concepts and
515 terminology. Agr. Ecosyst. Environ. 87, 111-117.
516 Jensen, J.L., Christensen, B.T., Schjønning, P., Watts, C.W., Munkholm, L.J., 2018. Converting
517 loss-on-ignition to organic carbon content in arable topsoil: Pitfalls and proposed procedure.
518 Eur. J. Soil Sci. (revised version submitted).
519 Jensen, J.L., Schjønning, P., Christensen, B.T., Munkholm, L.J., 2017a. Suboptimal fertilisation
520 compromises soil physical properties of a hard-setting sandy loam. Soil Res. 55, 332-340.
521 Jensen, J.L., Schjønning, P., Watts, C.W., Christensen, B.T., Munkholm, L.J., 2017b. Soil texture
522 analysis revisited: Removal of organic matter matters more than ever. PLOS ONE 12,
523 e0178039.
524 Johnston, A.E., 1972. The effect of ley and arable cropping systems on the amount of soil organic
525 matter in Rothamsted and Woburn Ley-Arable experiments. Report Rothamsted
526 Experimental Station for 1972, Part 2, 131-152.
527 Johnston, A.E., Poulton, P.R., Coleman, K., 2009. Chapter 1 Soil Organic Matter: Its Importance in
528 Sustainable Agriculture and Carbon Dioxide Fluxes. Adv. Agron. 101, 1-57.
529 Kalra, Y.P., Maynard, D.G., 1991. Methods manual for forest soil and plant analysis. Northern
530 Forestry Centre, Edmonton, Alberta.

Kay, B.D., Munkholm, L.J., 2004. Management-induced soil structure degradation - organic matter depletion and tillage. In: P. Schjønning, S. Elmholt, B.T. Christensen (Eds.), Managing Soil Quality: Challenges in Modern Agriculture. CABI Publishing, Wallingford, UK, 185-197.

Kenward, M.G., Roger, J.H., 2009. An improved approximation to the precision of fixed effects from restricted maximum likelihood. Comput. Stat. Data An. 53, 2583-2595.

Kleber, M., Eusterhues, K., Keiluweit, M., Mikutta, C., Mikutta, R., Nico, P.S., 2015. Mineral–Organic Associations: Formation, Properties, and Relevance in Soil Environments. Adv. Agron. 130, 1-140.

Le Bissonnais, Y., 1996. Aggregate stability and assessment of soil crustability and erodibility: I. Theory and methodology. Eur. J. Soil Sci. 47, 425-437.

Leifeld, J., 2006. Application of diffuse reflectance FT-IR spectroscopy and partial least-squares regression to predict NMR properties of soil organic matter. Eur. J. Soil Sci. 57, 846-857.

Matthews, G.P., Watts, C.W., Powlson, D.S., Price, J.C., Whalley, W.R., 2008. Wetting of agricultural soil measured by a simplified capillary rise technique. Eur. J. Soil Sci. 59, 817-823.

McNally, S.R., Beare, M.H., Curtin, D., Meenken, E.D., Kelliher, F.M., Calvelo Pereira, R., Shen, Q., Baldock, J., 2017. Soil carbon sequestration potential of permanent pasture and continuous cropping soils in New Zealand. Glob. Change Biol. 23, 4544-4555.

Oades, J.M., 1993. The role of biology in the formation, stabilization and degradation of soil structure. Geoderma 56, 377-400.

Peltre, C., Bruun, S., Du, C., Thomsen, I.K., Jensen, L.S., 2014. Assessing soil constituents and labile soil organic carbon by mid-infrared photoacoustic spectroscopy. Soil Biol. Biochem. 77, 41-50.

554 Peltre, C., Gregorich, E.G., Bruun, S., Jensen, L.S., Magid, J., 2017. Repeated application of
555 organic waste affects soil organic matter composition: Evidence from thermal analysis,
556 FTIR-PAS, amino sugars and lignin biomarkers. Soil Biol. Biochem. 104, 117-127.
557 Petersen, L.W., Moldrup, P., Jacobsen, O.H., Rolston, D.E., 1996. Relations between specific
558 surface area and soil physical and chemical properties. Soil Sci. 161, 9-21.
559 Pojasok, T., Kay, B.D., 1990. Assessment of a combination of wet sieving and turbidimetry to
560 characterize the structural stability of moist aggregates. Can. J. Soil Sci. 70, 33-42.
561 Pulido Moncada, M., Gabriels, D., Cornelis, W., Lobo, D., 2015. Comparing Aggregate Stability
562 Tests for Soil Physical Quality Indicators. Land Degrad. Dev. 26, 843-852.
563 Schjønning, P., de Jonge, L.W., Munkholm, L.J., Moldrup, P., Christensen, B.T., Olesen, J.E.,
564 2012. Clay dispersibility and soil friability—Testing the soil clay-to-carbon saturation
565 concept. Vadose Zone J. 11, 174-187.
566 Scott, T., Macdonald, A.J., Goulding, K.W.T., 2014. The UK Environmental Change Network,
567 Rothamsted. Physical and Atmospheric Measurements: The First 20 Years. Lawes
568 Agricultural Trust Co. Ltd., Harpenden.
569 Six, J., Conant, R.T., Paul, E.A., Paustian, K., 2002. Stabilization mechanisms of soil organic
570 matter: Implications for C-saturation of soils. Plant Soil 241, 155-176.
571 Sohi, S.P., Mahieu, N., Arah, J.R.M., Powlson, D.S., Madari, B., Gaunt, J.L., 2001. A Procedure for
572 Isolating Soil Organic Matter Fractions Suitable for Modeling. Soil Sci. Soc. Am. J. 65,
573 1121-1128.
574 Stewart, C.E., Paustian, K., Conant, R.T., Plante, A.F., Six, J., 2007. Soil carbon saturation:
575 concept, evidence and evaluation. Biogeochemistry 86, 19-31.
576 Tisdall, J.M., Oades, J.M., 1982. Organic matter and water-stable aggregates in soils. J. Soil Sci.
577 33, 141-163.

578 Toms, J.D., Lesperance, M.L., 2003. Piecewise regression: A tool for identifying ecological
579 thresholds. Ecology 84, 2034-2041.
580 Villada, A., Vanguelova, E.I., Verhoef, A., Shaw, L.J., 2016. Effect of air-drying pre-treatment on
581 the characterization of forest soil carbon pools. Geoderma 265(Supplement C), 53-61.
582 Watts, C.W., Dexter, A.R., 1997. The influence of organic matter in reducing the destabilization of
583 soil by simulated tillage. Soil Tillage Res. 42, 253-275.
584 Weil, R.R., Islam, K.R., Stine, M.A., Gruver, J.B., Samson-Liebig, S.E., 2003. Estimating active
585 carbon for soil quality assessment: A simplified method for laboratory and field use. Am. J.
586 Alternative Agr. 18, 3-17.
587
588

589 **Figure captions**

590 **Fig. 1.** Distribution of plots in Highfield showing the arable (A), ley-arable (LA) and grass (G)
591 treatments in blocks 1-4 of the ley-arable experiment, and the bare fallow (BF) treatment in blocks
592 1-3 of the bare fallow experiments.

593 **Fig. 2.** (a) Permanganate oxidizable carbon (POXC) as a function of SOC and (b) hot water-
594 extractable carbon (HWC) as a function of SOC for the four treatments at subplot level. The
595 broken-stick and linear regression models are indicated.

596 **Fig. 3.** Principal component analysis (PCA) based on FTIR-PAS spectra for the different
597 treatments. The dots indicate the four plots of each treatment. For treatment abbreviations, see Fig.
598 1. (a) Scores plot in the plane defined by principal component 1 (PC1, explaining 84.6% of the
599 variance) and principal component 2 (PC2, explaining 7.5% of the variance) of the PCA. (b)
600 Loadings of the PCA for PC1 and PC2.

601 **Fig. 4.** Clay dispersibility of 1-2 mm aggregates rewetted to -100 hPa (solid lines) and
602 disintegration (the ratio between clay content estimated without SOM removal and with removal)
603 (dashed lines) as a function of (a) soil organic carbon (SOC), (b) permanganate oxidizable carbon
604 (POXC), and (c) hot water-extractable carbon (HWC) for the four treatments at subplot level. The
605 broken-stick models (Table 3) are indicated. See Table 3 for equations and R^2-values.

606 **Fig. 5.** (a) Clay dispersibility and (b) Clay-SOM disintegration as a function of soil organic carbon
607 (SOC; black symbols) and LF-free-SOC (Light fraction-free-SOC; white symbols). The broken-
608 stick models and R^2-values are indicated.

609 **Fig. 6.** (a) The ratio between dispersed particles <20 μm and the total content of particles <20 μm as
610 a function of Log10(min) at treatment level. The standard error of the mean is indicated (n=4). The

611 polynomials are fitted to the four replicates time's seven data points per treatment. Letters denote
612 statistical significance at $P<0.05$ for the comparison of A, LA and G. An asterisk (*) indicates if BF
613 is significantly different from A, LA and G based on a pairwise *t*-test. (b) Release rate (kg kg^{-1}
614 minerals dispersed min^{-1}) as a function of Log10(min) at treatment level. A stepwise, simple
615 calculation of slope from time step to time step was employed to calculate the release rate, and a
616 smoothed spline curve was added.

617

618 **Table 1** Soil characteristics. Within rows, letters denote statistical significance at $P<0.05$ for the
619 comparison of A, LA and G. An asterisk (*) indicates if BF is significantly different from A, LA
620 and G based on a pairwise *t*-test. For treatment abbreviations, see Fig. 1.

	BF	A	LA	G
Texture[a]				
Clay <2 μm	0.270	0.264	0.255	0.261
Silt 2-20 μm	0.249	0.263	0.261	0.272*
Silt 20-63 μm	0.335	0.318	0.324	0.319
Sand 63-2000 μm	0.146	0.155	0.160	0.148
Specific surface area (m^2 g^{-1} minerals)[b]	56.7	67.9[a*]	68.4[a*]	78.4[b*]
Exchangeable cations and CEC				
Na^+ ($mmol_c$ kg^{-1} minerals)	0.4	0.5[a]	0.4[a]	0.7[b*]
K^+ ($mmol_c$ kg^{-1} minerals)	3.3	6.3	17.7	5.8
Ca^{2+} ($mmol_c$ kg^{-1} minerals)	93.7	113.3[a]	128.7[a]	155.6[b*]
Mg^{2+} ($mmol_c$ kg^{-1} minerals)	5.4	4.0	4.1	4.6
Sum of bases ($mmol_c$ kg^{-1} minerals)	102.9	107.1[a]	120.7[ab]	142.0[b*]
CEC ($mmol_c$ kg^{-1} minerals)	145.8	173.8	171.3	209.9*
Base saturation (%)	72.8	65.5	74.8	74.4
pH ($CaCl_2$)	5.7	5.1	5.1	5.4

621 [a]kg kg^{-1} of mineral fraction and based on oven-dry weight.

622 [b]Clay is included as a co-variable since it is significant in itself and makes the treatment effect
623 significant.

624

Table 2 Soil organic matter characteristics, clay dispersibility of 1-2 mm aggregates rewetted to -100 hPa and clay-SOM disintegration (the ratio between clay content estimated without SOM removal and with removal). Within rows, letters denote statistical significance at $P<0.05$ for the comparison of A, LA and G. An asterisk (*) indicates if BF is significantly different from A, LA and G based on a pairwise *t*-test. For treatment abbreviations, see Fig. 1.

	BF	A	LA	G
Soil organic matter characteristics				
Soil organic carbon (SOC, kg kg^{-1} minerals)	0.0090	0.0173^{a*}	0.0216^{a*}	0.0329^{b*}
Permanganate oxidizable carbon (POXC, g kg^{-1} minerals)	0.161	0.458^{a*}	0.600^{b*}	0.818^{c*}
% of SOC	1.7	2.6^{ab*}	2.8^{b*}	2.5^{a*}
Hot water-extractable carbon (HWC, g kg^{-1} minerals)	0.437	0.777^{a*}	1.082^{b*}	1.611^{c*}
% of SOC	4.6	4.5^{a}	5.0^{b}	4.9^{ab}
Light fraction carbon (LFSOC, g kg^{-1} minerals)	0.167	1.285^{a*}	1.732^{a*}	2.579^{b*}
% of SOC	1.9	7.4*	8.0*	7.8*
Aliphatic peak area	58	99^{a*}	121^{a*}	159^{b*}
Aliphatic peak area/SOC	65	57	56	49*
Soil structural stability				
Clay dispersibility (DispClay, kg kg^{-1} minerals)	0.0115	0.0074^{c*}	0.0051^{b*}	0.0034^{a*}
Clay-SOM disintegration (DI, kg kg^{-1} minerals)	1.02	0.96^{b}	1.00^{b}	0.74^{a*}

Table 3 Parameters of the linear, semi-logarithmic and broken-stick models for clay dispersibility (DispClay; kg kg^{-1} minerals) and clay-SOM disintegration (DI; kg kg^{-1} minerals) as a function of soil organic carbon (SOC; kg kg^{-1} minerals), permanganate oxidizable carbon (POXC; g kg^{-1} minerals), and hot water-extractable carbon (HWC; g kg^{-1} minerals). The change point of the broken-stick model and the corresponding 95% confidence interval is indicated. The relation between the first and second slope estimate of the broken-stick model (Slope1/Slope2) was calculated if both slopes were significant. The coefficient of determination (R^2) is indicated.

Predictor	Model		Equation	Change point	Slope1/Slope2	R^2
SOC	Linear	DispClay	0.0134^{***}-0.32^{***} SOC			0.839
		DI	1.16^{***}-11.6^{***} SOC			0.723
	Semi-log	DispClay	-0.0189^{***} -0.0148^{***} log(SOC)			0.930
		DI	0.16^{***} -0.442^{***} log(SOC)			0.555
	Broken-stick	DispClay	0.0160^{***}-0.49^{***} SOC + 0.39^{***} $(SOC-0.0235)^{+}$	0.0235^{***} [0.0209:0.0260]	4.6	0.940
		DI	1.03^{***}-2.9^{NS} SOC – 18.0^{***} $(SOC-0.0225)^{+}$	0.0225^{***} [0.0199:0.0251]		0.880
POXC	Linear	DispClay	0.0131^{***}-0.0122^{***} POXC			0.907
		Di	1.11^{***}-0.366^{***} POXC			0.550
	Semi-log	DispClay	0.0029^{***} -0.011^{***} log(POXC)			0.891
		DI	0.83^{***} -0.261^{***} log(POXC)			0.364
	Broken-stick	DispClay	0.0136^{***}-0.0138^{***} POXC + 0.0084^{*} $(POXC-0.694)^{+}$	0.694^{*} [0.564:0.824]	2.6	0.927
		DI	1.02^{***}-0.087^{NS} POXC - 1.00^{***} $(POXC-0.628)^{+}$	0.628^{***} [0.573:0.683]		0.819
HWC	Linear	DispClay	0.0128^{***}-0.0061^{***} HWC			0.815
		DI	1.13^{***}-0.21^{***} HWC			0.648
	Semi-log	DispClay	0.0059^{***} -0.0133^{***} log(HWC)			0.900
		DI	0.90^{***}-0.378^{***} log(HWC)			0.490
	Broken-stick	DispClay	0.0156^{***}-0.0105^{***} HWC + 0.00760^{***} $(HWC-0.970)^{+}$	0.970^{***} [0.833:1.107]	3.6	0.913
		DI	1.02^{***}-0.049^{NS} HWC – 0.341^{***} $(HWC-1.104)^{+}$	1.104^{***} [0.921:1.288]		0.788

637 * and *** indicate significance level at $P<0.05$ and $P<0.001$, respectively.

638 NS: Not significant.

639 +: Indicates that the last term is valid only when the content of SOC, POXC or HWC are larger than the change point.

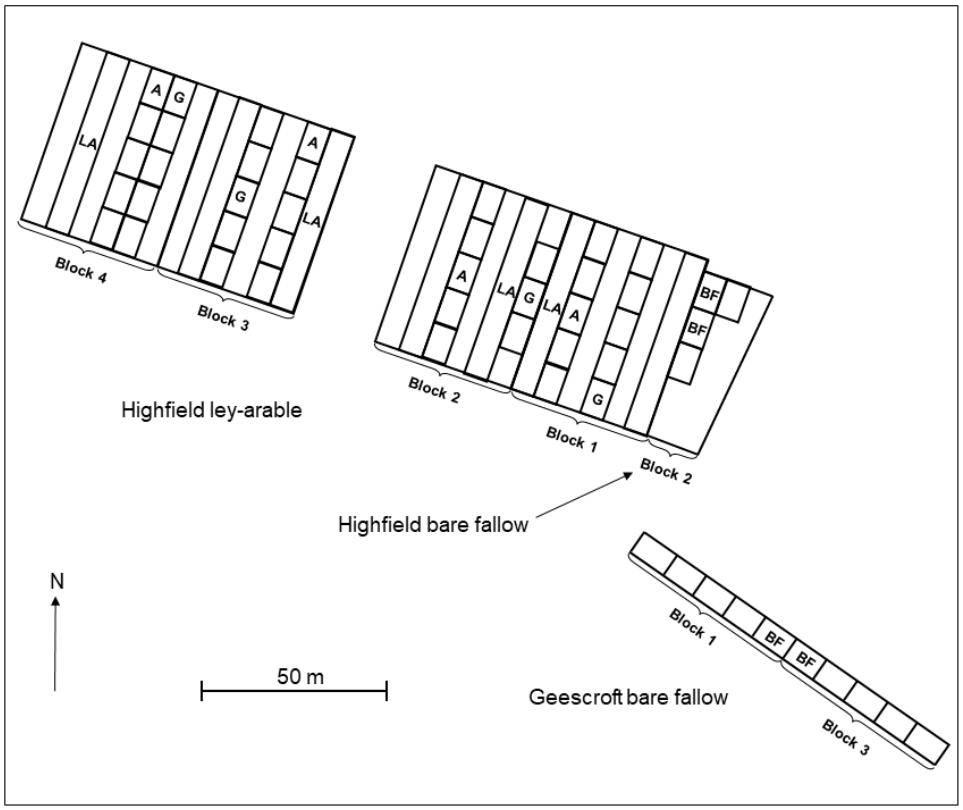

640

641 **Fig. 1.** Distribution of plots in Highfield showing the arable (A), ley-arable (LA) and grass (G)
642 treatments in blocks 1-4 of the ley-arable experiment, and the bare fallow (BF) treatment in blocks
643 1-3 of the bare fallow experiments.

644

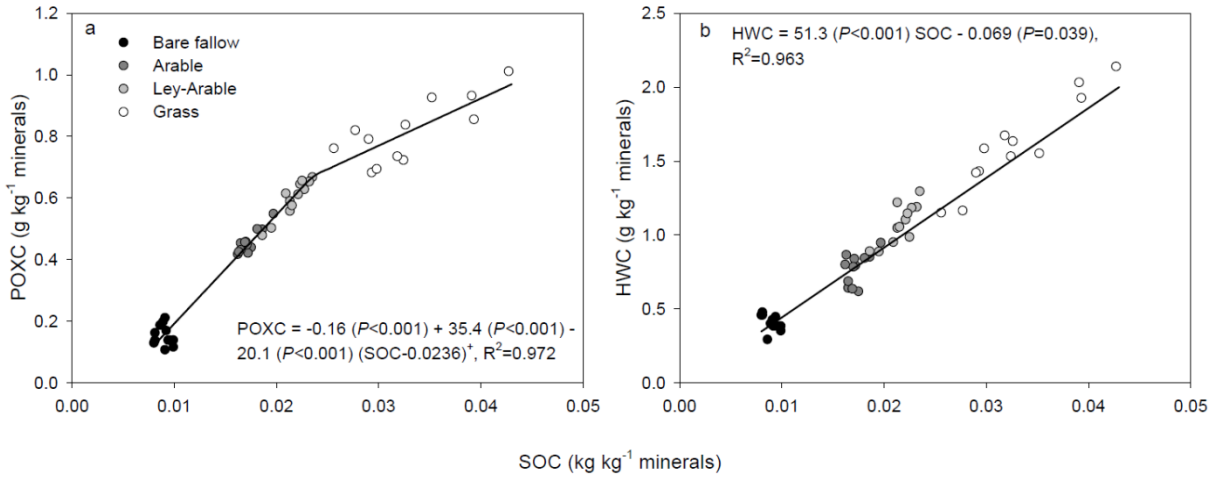

645

646 **Fig. 2.** (a) Permanganate oxidizable carbon (POXC) as a function of SOC and (b) hot water-
647 extractable carbon (HWC) as a function of SOC for the four treatments at subplot level. The
648 broken-stick and linear regression models are indicated.

649

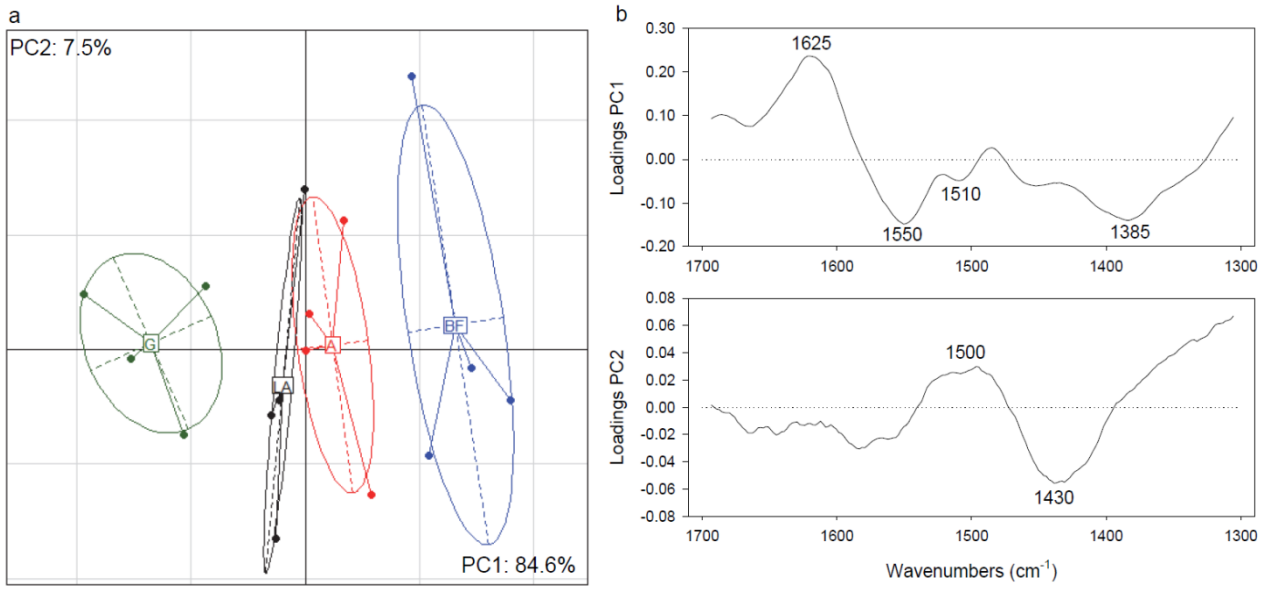

650

651 **Fig. 3.** Principal component analysis (PCA) based on FTIR-PAS spectra for the different

652 treatments. The dots indicate the four plots of each treatment. For treatment abbreviations, see Fig.

653 1. (a) Scores plot in the plane defined by principal component 1 (PC1, explaining 84.6% of the

654 variance) and principal component 2 (PC2, explaining 7.5% of the variance) of the PCA. (b)

655 Loadings of the PCA for PC1 and PC2.

656

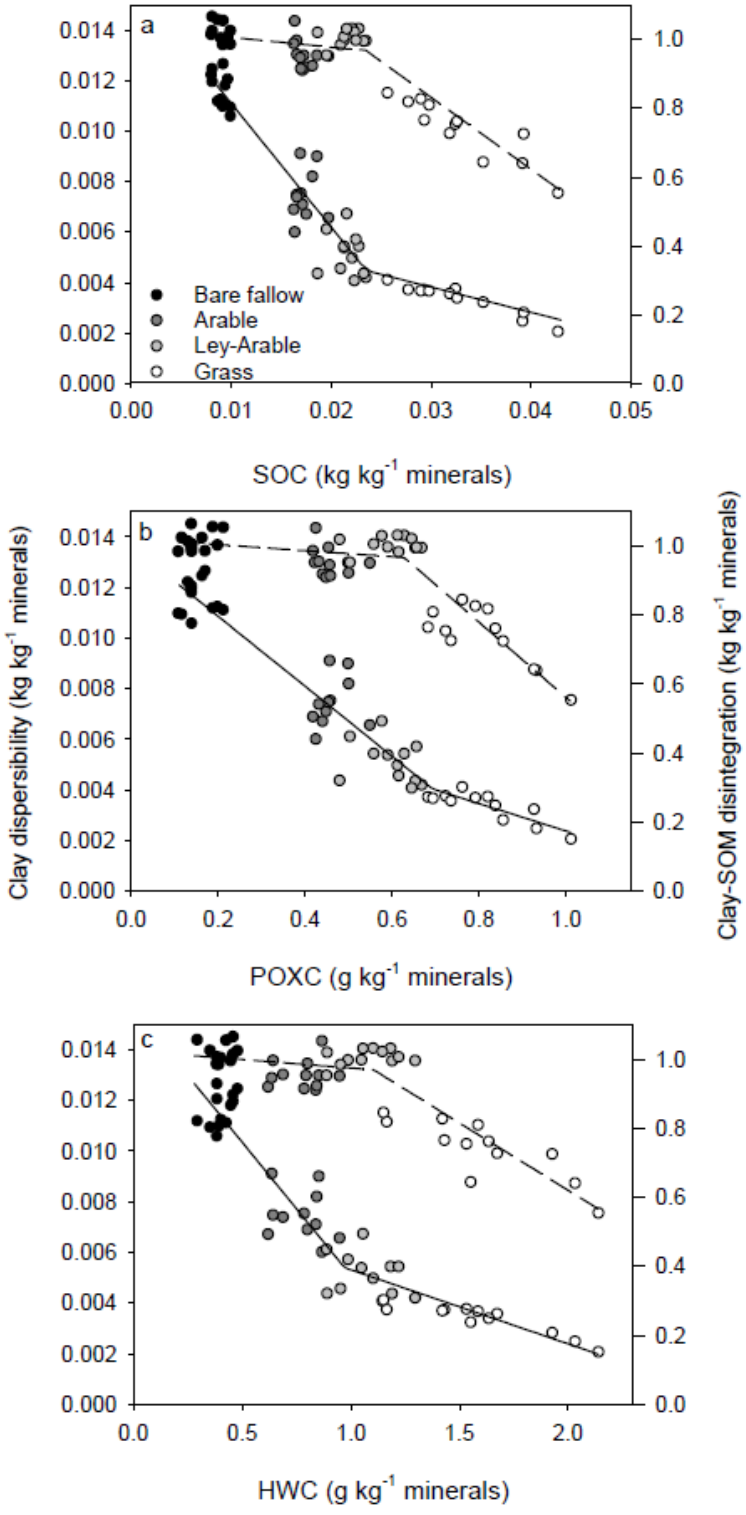
a
b
c
Bare fallow
Arable
Ley-Arable
Grass
SOC (kg kg-1 minerals)
POXC (g kg-1 minerals)
HWC (g kg-1 minerals)
Clay dispersibility (kg kg-1 minerals)
Clay-SOM disintegration (kg kg-1 minerals)

657

658

Fig. 4. Clay dispersibility of 1-2 mm aggregates rewetted to -100 hPa (solid lines) and clay-SOM disintegration (the ratio between clay content estimated without SOM removal and with removal) (dashed lines) as a function of (a) soil organic carbon (SOC), (b) permanganate oxidizable carbon (POXC), and (c) hot water-extractable carbon (HWC) for the four treatments at subplot level. The broken-stick models (Table 3) are indicated. See Table 3 for equations and R^2-values.

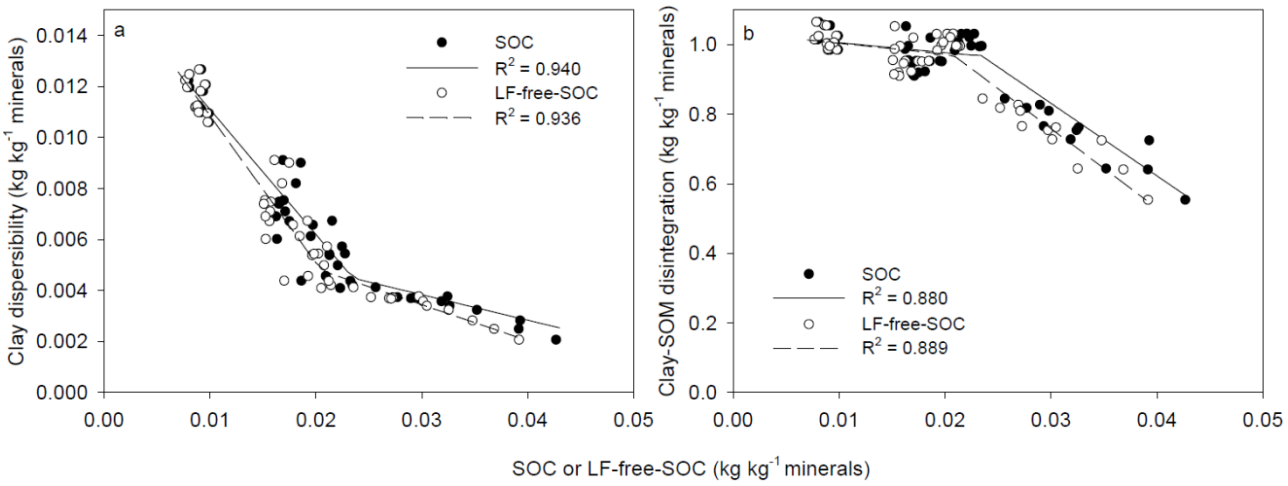

665

666 **Fig. 5.** (a) Clay dispersibility of 1-2 mm aggregates rewetted to -100 hPa and (b) Clay-SOM
667 disintegration (the ratio between clay content estimated without SOM removal and with removal) as
668 a function of soil organic carbon (SOC; black symbols) and LF-free-SOC (Light fraction-free-SOC;
669 white symbols). The broken-stick models and R^2-values are indicated.

670

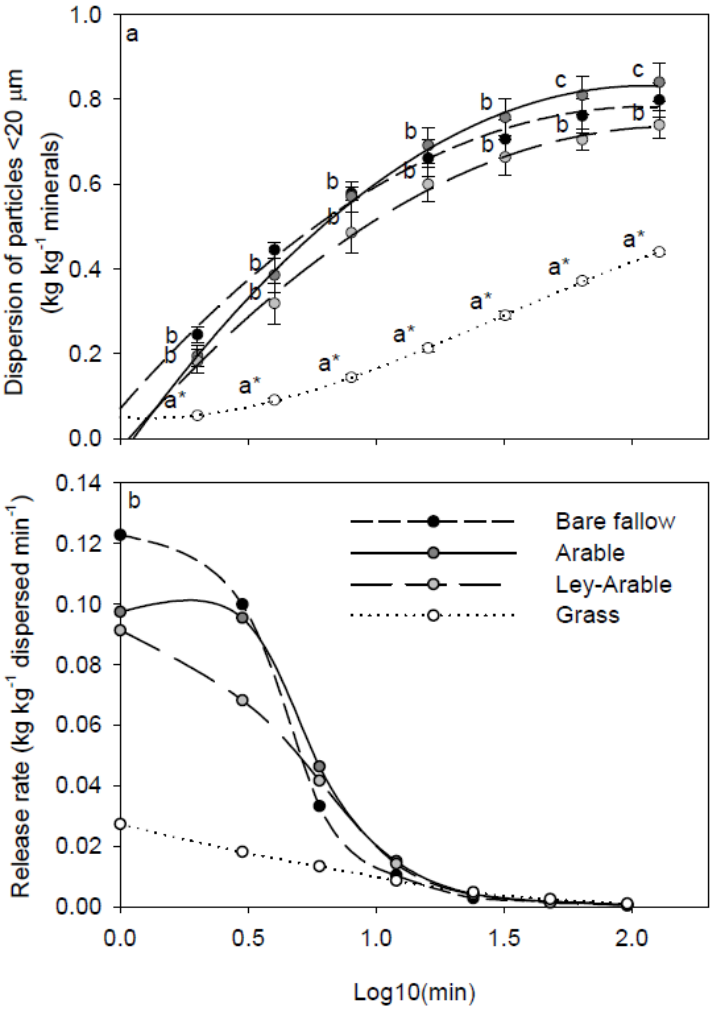

671

672 **Fig. 6.** (a) The ratio between dispersed particles <20 µm and the total content of particles <20 µm as
673 a function of Log10(min) at treatment level. The standard error of the mean is indicated (n=4). The
674 polynomials are fitted to the four replicates time's seven data points per treatment. Letters denote
675 statistical significance at P<0.05 for the comparison of A, LA and G. An asterisk (*) indicates if BF
676 is significantly different from A, LA and G based on a pairwise t-test. (b) Release rate (kg kg^{-1}
677 minerals dispersed min^{-1}) as a function of Log10(min) at treatment level. A stepwise, simple
678 calculation of slope from time step to time step was employed to calculate the release rate, and a
679 smoothed spline curve was added.

Supplementary material for the article entitled: ”Relating soil C and organic matter fractions to structural stability” by Jensen et al.

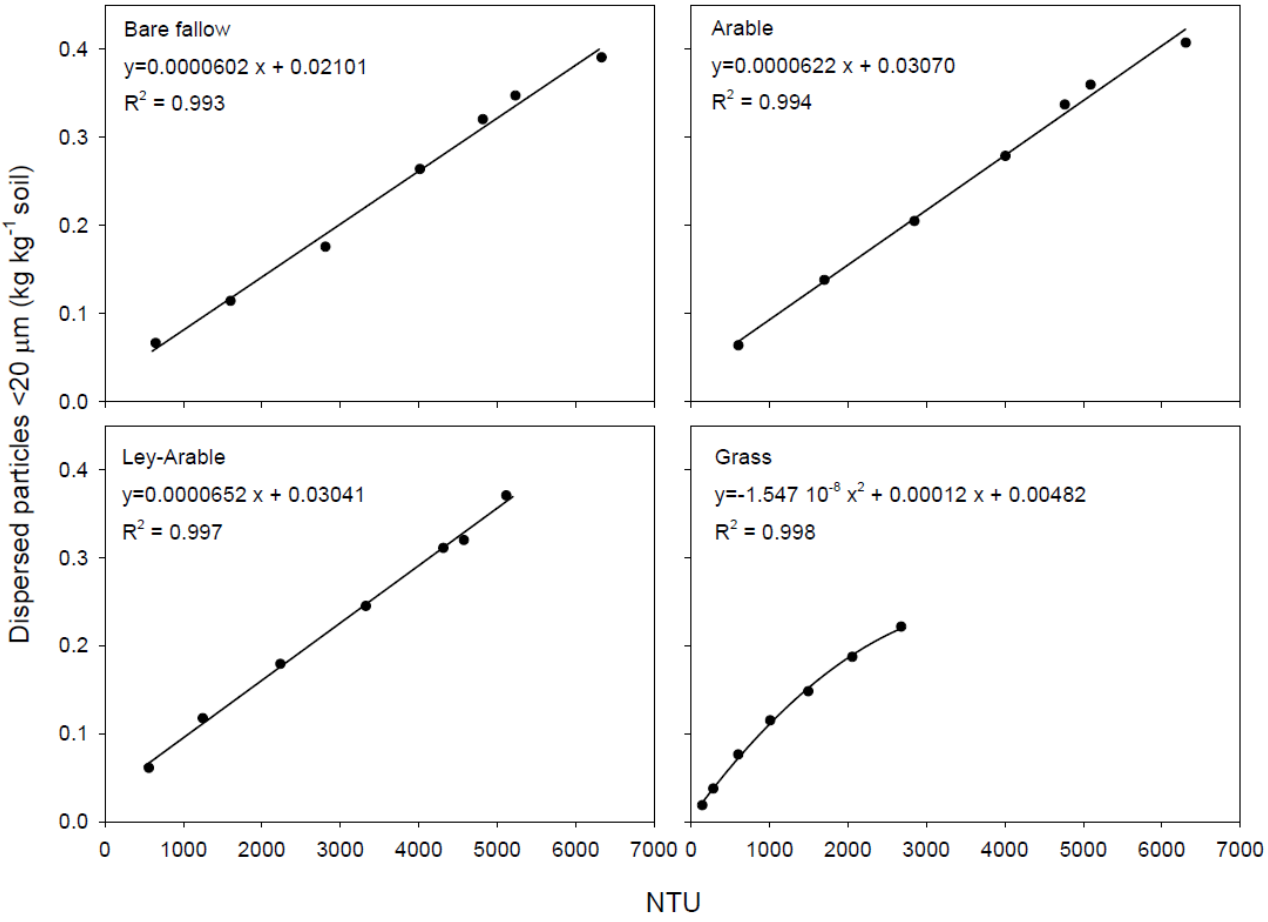

Fig. S1. The correlation between nephelometric turbidity (NTU) and dispersed particles <20 µm (kg kg^{-1} soil) for the four different treatments.

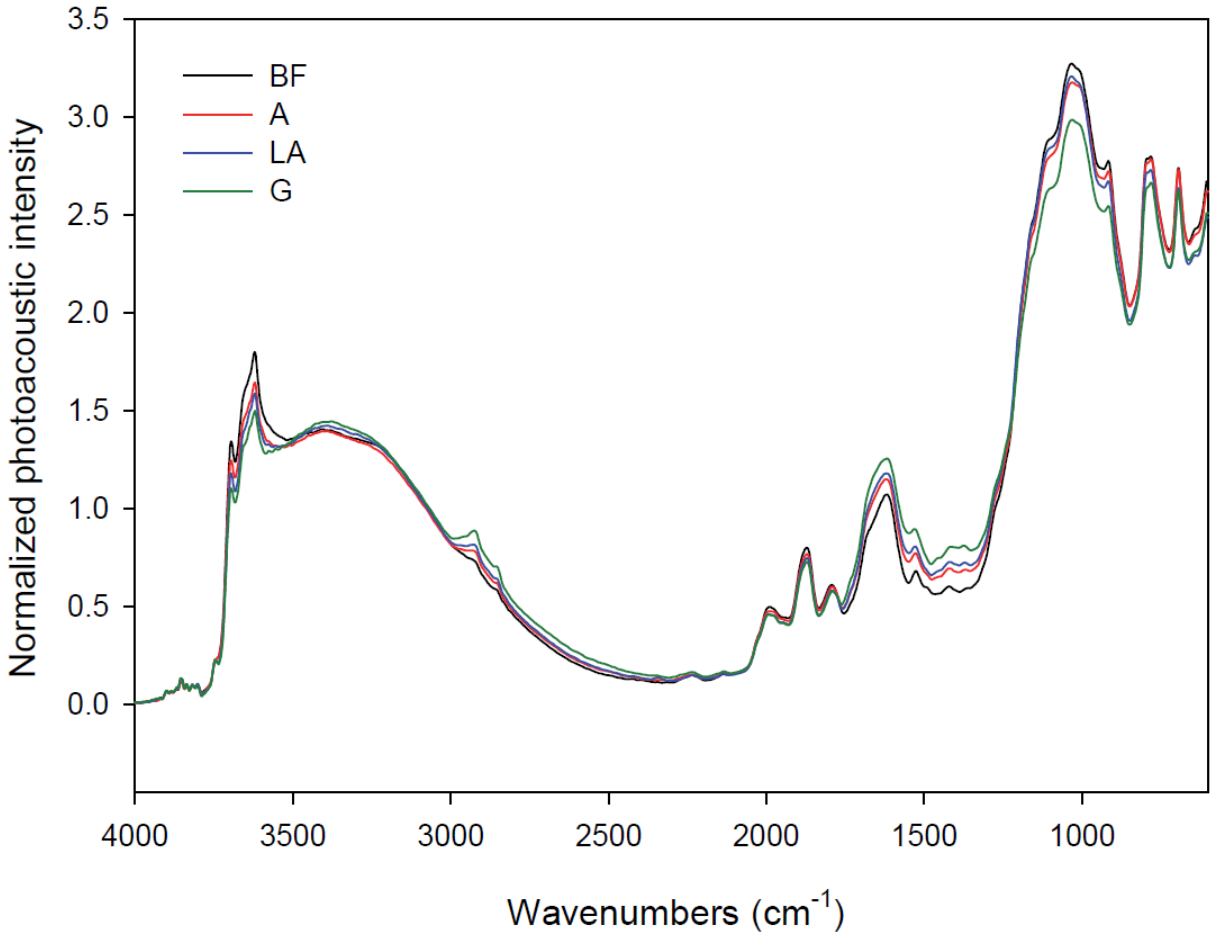

Fig. S2. Spectra of the different treatments from Highfield over the selected FTIR region 4000-600 cm^{-1}. The spectra are presented as the average of the spectra from the four field plots. BF, Bare fallow; A, Arable; LA, Ley-arable; G, Grass.

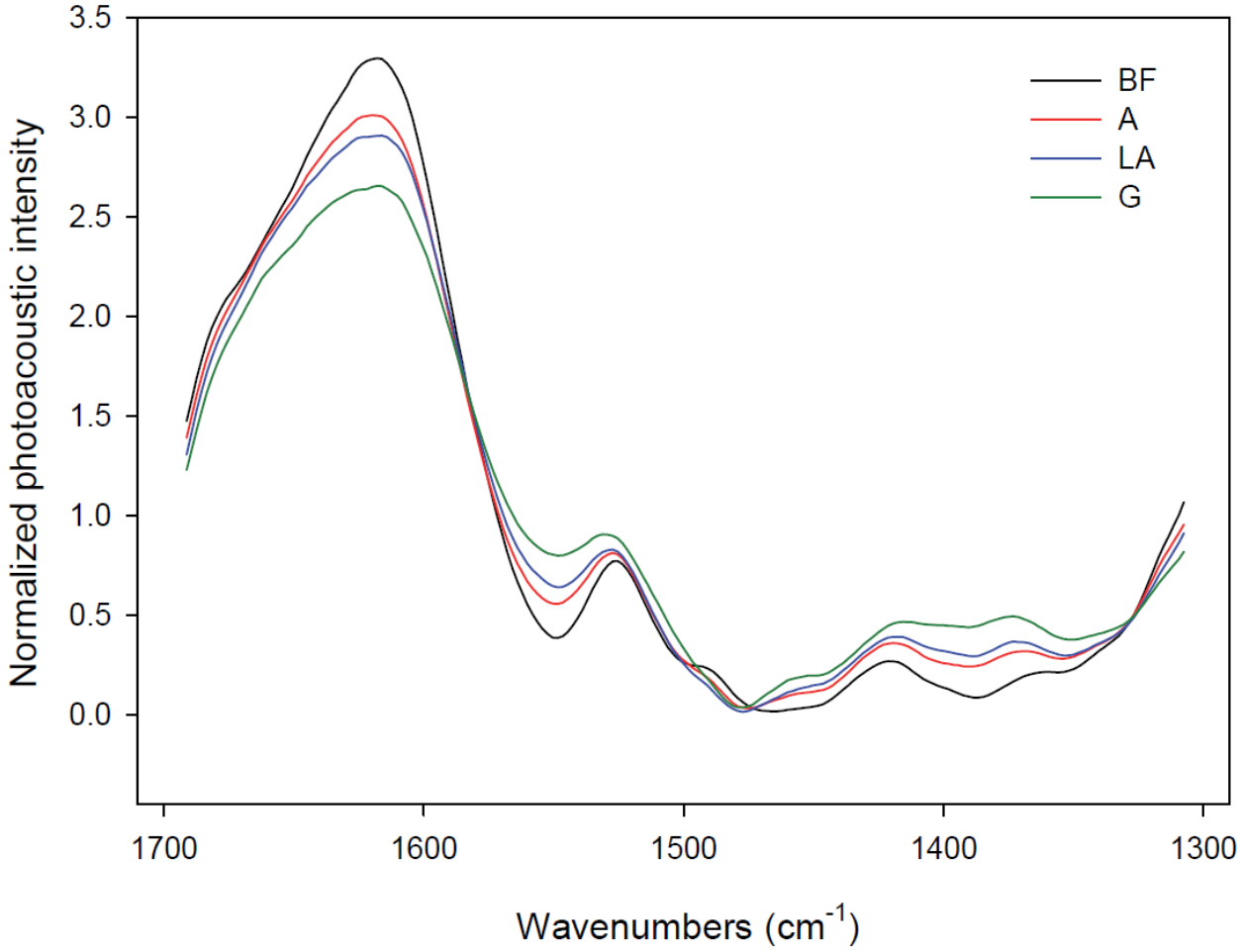

Fig. S3. Spectra of the different treatments from Highfield over the selected FTIR region 1700-1300 cm^{-1}. The spectra are presented as the average of the spectra from the four field plots. BF, Bare fallow; A, Arable; LA, Ley-arable; G, Grass.

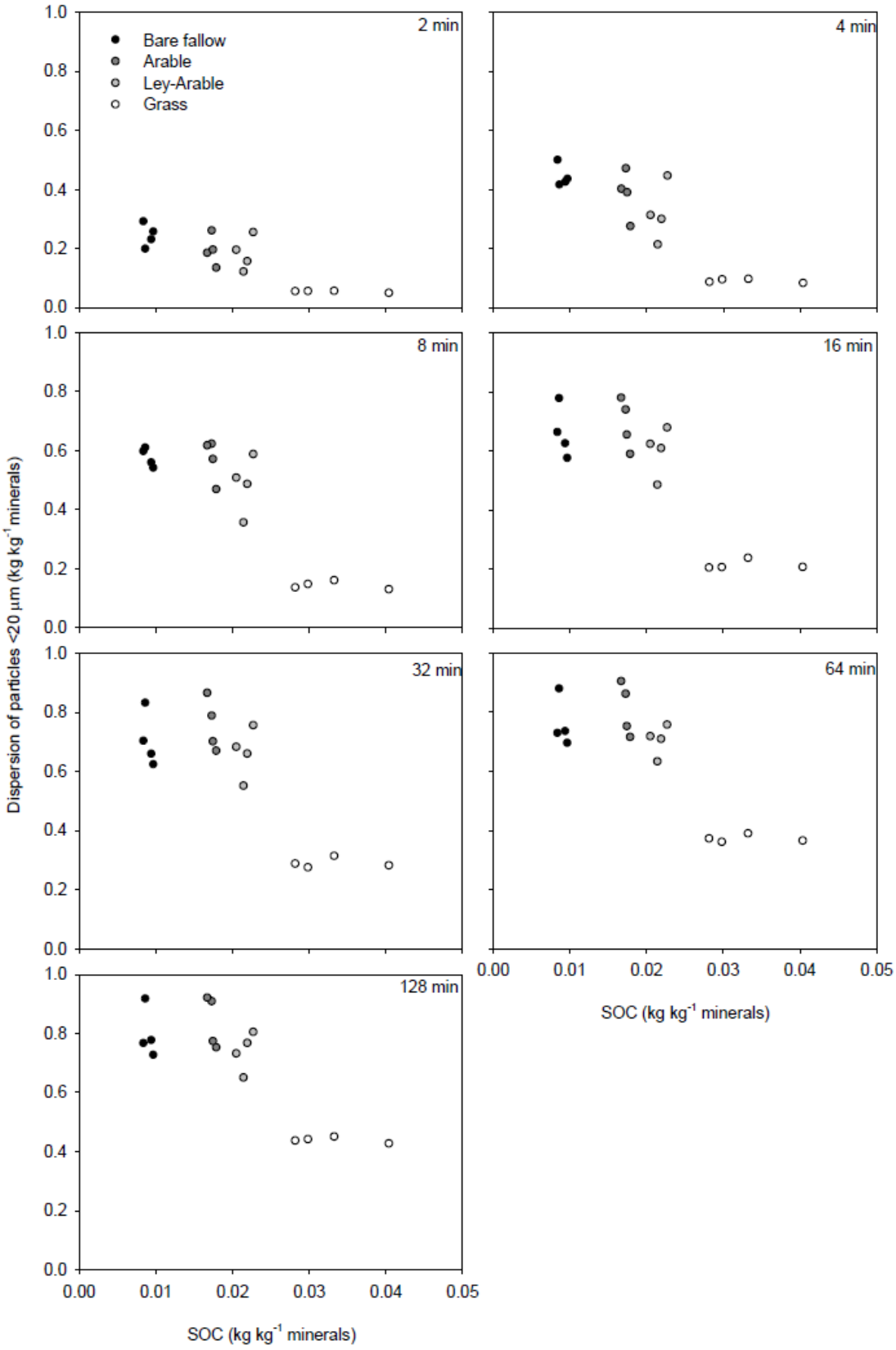

Fig. S4. The ratio between dispersed particles <20 µm and the total content of particles <20 µm as a function of soil organic carbon at plot level for the seven time steps.